

Fast Low-Angle Positive-Contrast Imaging with Alternating Repetition Time SSFP

T. Çukur¹, W. Overall¹, and D. G. Nishimura¹

¹Electrical Engineering, Stanford University, Stanford, CA, United States

Introduction: There has been recent interest in methods that provide positive contrast from susceptibility-induced field variations [1-3]. These methods can be used for tracking of interventional devices or imaging of super paramagnetic iron oxide (SPIO)-labeled cells. Fast low-angle positive-contrast SSFP (FLAPS) [4] is an imaging method that uses the low-tip-angle bSSFP profile to reduce on-resonant signal, and provides low specific absorption rates (SAR) and inherent flow insensitivity. However, the level of suppression and achievable positive contrast are limited. In this work, we propose the use of alternating repetition time (ATR) SSFP [5] to create an improved stop-band centered at the water resonance. Compared to FLAPS, the ATR sequence achieves more robust background suppression and is shown to increase the range of flip angles that produce positive contrast.

Methods: ATR SSFP creates a broad stop-band around a central null using two consecutive repetition times, TR1 and TR2 as shown in Fig.1.a. The width of this stop-band is inversely proportional to the total TR, TR1+TR2. The null can be aligned with a certain frequency if the phase acquired due to free precession within TR2 at this frequency is equal to the phase of RF2, ϕ_2 . Therefore, on-resonant suppression can be achieved for $\phi_2 = 0^\circ$. It is important to note that this stop-band is achieved regardless of the flip angle and the T1/T2 ratio. The central null has exactly zero signal even for very high flip angles, in contrast to regular bSSFP. The magnetization profiles for bSSFP and ATR are displayed in Fig.1 for a range of flip angles. ATR achieves better suppression than bSSFP for all flip angles.

The level of background suppression can be quantified by the peak contrast (difference of the peak signal around the bSSFP null and the signal at on-resonance) [4]. However, the signal in the ATR stop-band varies and there is always a perfect null point. Therefore, it is more appropriate to compute the peak contrast using an average on-resonance signal (over $3\pi/2$ radians/TR). Figure 2 shows that ATR SSFP outperforms FLAPS in terms of contrast over a broad range of flip angles and T1/T2 ratios. The average contrast improvement over FLAPS is 127 %.

Results: The enhanced on-resonant suppression of ATR SSFP was demonstrated with phantom (T1/T2=250/50 ms) images (Fig.3). A linear shim was applied horizontally. $\alpha=5^\circ$ and a total TR of 3.9 ms were used for both sequences, yielding equivalent central stop-band widths of 256 Hz. 2D GRE, 3D FLAPS and 3D ATR SSFP images of an SPIO phantom were acquired on a 1.5 T GE Excite scanner (Fig.4). The acquisition parameters were: $\alpha=5^\circ$, TR1/TR2=3.3/0.6 ms for ATR and TR=3.9 ms for FLAPS, 14 cm FOV, $0.88 \times 0.88 \times 4 \text{ mm}^3$ resolution, $\pm 62.5 \text{ kHz}$ BW, and an acquisition time of 0:13 for both. For the GRE sequence: $\alpha=30^\circ$, TR=20 ms, BW= $\pm 31.3 \text{ kHz}$. ATR SSFP significantly reduces the on-resonant signal.

Conclusion: Low angle ATR SSFP is a fast imaging technique that produces positive contrast from susceptibility-induced field variations with virtually no background signal from on-resonant spins. It has low SAR and flow sensitivity. Furthermore, enhanced positive contrast over a wider range of tip angles and T1/T2 ratios extend the applicability of the method compared to FLAPS.

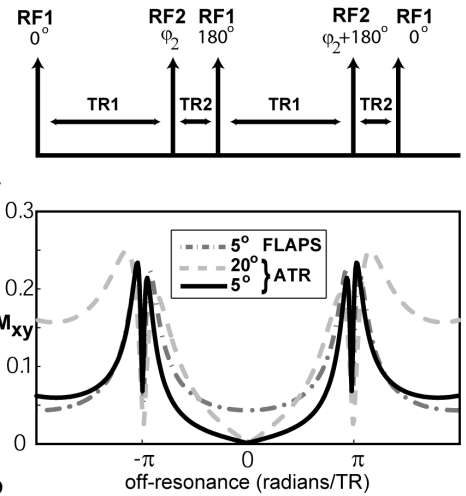


Figure 1. a: ATR sequence where the labels indicate the RF phases and all pulses have the same tip angle α . **b:** FLAPS ($\alpha=5^\circ$) and ATR ($\alpha=5^\circ, 20^\circ$) profiles.

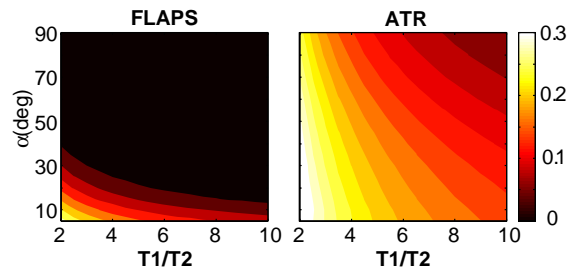


Figure 2. Peak contrast for FLAPS and ATR. ATR achieves higher contrast for all T1/T2 ratios and α .

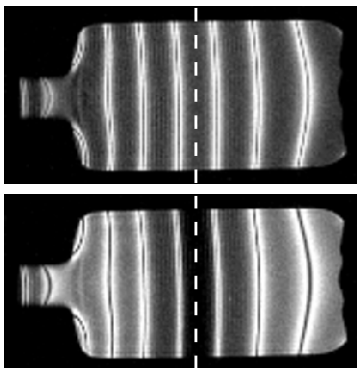


Figure 3. Phantom images acquired with FLAPS (top) and ATR SSFP (bottom). The vertical line is the water-resonance. A horizontal linear shim was applied. ATR improves on-resonant suppression.

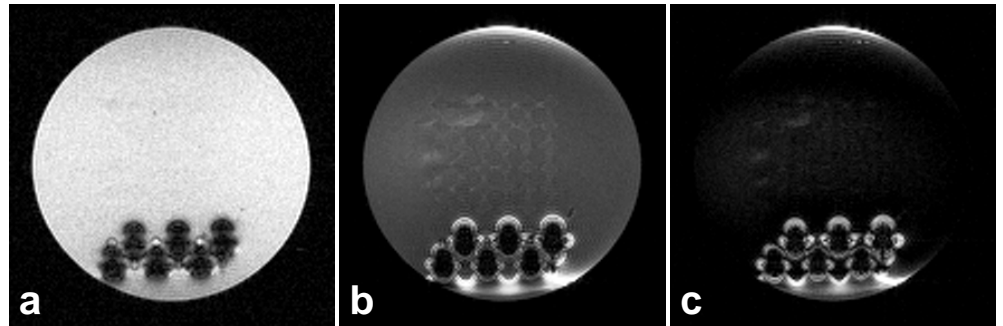


Figure 4. SPIO phantom (6 labeled-tubes) images acquired with **a:** GRE, **b:** FLAPS and **c:** ATR. ATR achieves superior background suppression. Identical display windowing was used for **b** and **c**.

References:

1. Cunningham *et al.* MRM 55, 2005.
2. Wacker, *et al.* MRI Clin N Am 13, 2005.
3. Bulte and Kraitchmann, NMR in Biomed 17, 2004.
4. Dharmakumar, *et al.* Phys Med Biol 51, 2006.
5. Leupold, *et al.* MRM 55, 2006.